

# Three-Dimensional Distance and Coverage Maps in the Assessment of Peritalar Subluxation in Progressive Collapsing Foot Deformity

Kevin N. Dibbern, PhD<sup>1</sup> , Shuyuan Li, MD, PhD<sup>1</sup>, Victoria Vivtcharenko, BS<sup>1</sup>, Elijah Auch, MS<sup>1</sup>, Francois Lintz, MD, MSc, FEBOT<sup>2</sup> , Scott J. Ellis, MD<sup>3</sup> , John E. Femino, MD<sup>1</sup>, and Cesar de Cesar Netto, MD, PhD<sup>1</sup> 

Foot & Ankle International®

2021, Vol. 42(6) 757–767

© The Author(s) 2021

Article reuse guidelines:

sagepub.com/journals-permissions

DOI: 10.1177/1071100720983227

journals.sagepub.com/home/fai

## Abstract

**Background:** Progressive collapsing foot deformity (PCFD), formerly termed *adult-acquired flatfoot deformity*, is a complex 3-dimensional (3D) deformity of the foot characterized by peritalar subluxation (PTS). PTS is typically measured at the posterior facet, but recent studies have called this into question. The objective of this study was to use 3D distance mapping (DM) from weightbearing computed tomography (WBCT) to assess PTS in patients with PCFD and controls. We hypothesized that DMs would identify the middle facet as a superior marker for PTS.

**Methods:** We analyzed WBCT data of 20 consecutive stage I patients with PCFD and 10 control patients with a novel DM technique to objectively characterize joint coverage across the entire peritalar surface, including both articular and nonarticular regions. Joint coverage was defined as the percentage of articular area with DMs <4 mm and impingement when distances were <0.5 mm. Comparisons were performed with independent *t* tests or Wilcoxon tests. *P* values <.05 were considered significant.

**Results:** Overall, coverage was decreased in articular regions and impingement was increased in nonarticular regions of patients with PCFD with a significant increase in uncoverage in the middle (46.6%, *P* < .001) but not anterior or posterior facets. Significant increases in sinus tarsi coverage were identified (98.0%, *P* < .007) with impingement in 6 of 20 patients with PCFD. Impingement of the subfibular region was noted in only 1 of 20 cases but narrowing greater than 2 standard deviations was noted in 17 of 20 patients.

**Conclusion:** Objective DMs identified significant markers of PTS in the middle but not posterior or anterior facets. We confirmed prior 2-dimensional data that suggested uncoverage of the middle facet provided a more robust and consistent measure of PTS than measures in the posterior facet.

**Level of Evidence:** Level III, case-control study.

**Keywords:** progressive collapsing foot deformity, PCFD, flatfoot, distance maps, weightbearing CT, WBCT, peritalar subluxation, PTS

Progressive collapsing foot deformity (PCFD), formerly termed *adult-acquired flatfoot deformity*,<sup>1,5</sup> is a complex 3-dimensional (3D) multifocal and multiplanar pathology characterized by peritalar subluxation (PTS) of the hindfoot through the triple joint complex.<sup>9,27,29</sup> Historically, conventional 2-dimensional (2D) weightbearing radiographs have been used to assess the articular component and alignment of this deformity.<sup>14,15,25,26,31</sup> More recently, weightbearing computed tomography (WBCT) has become widely used to identify and optimize staging of many foot and ankle conditions, including PCFD,<sup>1,3,6,7,11,12,16-18,24,28</sup> enabling improved assessment of the coronal plane component of

PTS and hindfoot deformity,<sup>1,5,30</sup> including the inherently increased valgus anatomy of the subtalar joint (SJ)<sup>6,7,12,21,28</sup>

<sup>1</sup>Department of Orthopedics and Rehabilitation, University of Iowa, Iowa City, IA, USA

<sup>2</sup>Ramsay GDS-Clinique de L'Union, Saint Jean, France

<sup>3</sup>The Hospital for Special Surgery, New York, NY, USA

## Corresponding Author:

Cesar de Cesar Netto, MD, PhD, Department of Orthopaedic and Rehabilitation, University of Iowa, 200 Hawkins Drive, Iowa City, IA 52242-1091, USA.

Email: cesardecesarnetto@uiowa.edu

and presence of sinus tarsi (ST) and subfibular (SF) impingements.<sup>16,24</sup>

PTS has been shown to occur with early symptomatic PCFD, and quantifying it provides a means to objectively characterize deformity progression. The first report gauging PTS was by Ananthakrisnan et al,<sup>1</sup> who demonstrated subluxation in all 3 SJ articular facets of patients with PCFD compared to controls, using coronal plane–simulated WBCT images.<sup>10</sup> Subsequently, multiple authors have studied PTS using subluxation of the posterior facet of the SJ as a marker of deformity.<sup>6,10,12,13,16,17,21,28</sup> However, recently, de Cesar Netto et al<sup>10</sup> proposed subluxation of the SJ middle facet as a better marker of pronounced PTS. They demonstrated high diagnostic accuracy for symptomatic PCFD when measuring middle facet joint uncoverage and incongruence in a single coronal plane image at the anteroposterior midpoint of the articular facet. Their subsequent study then provided evidence that PTS measures in the middle facet show more pronounced subluxation than the posterior facet.<sup>14</sup>

The objective of this study was to apply the concepts of PTS in patients with PCFD in a full 3D setting where the whole extension of the SJ and peritalar interface can be assessed rather than a single coronal plane measurement of the articular facet. To accomplish this, we leverage distance mapping (DM), a recently validated, objective 3D tool that evaluates joint space in the foot and ankle across entire bony interfaces by obtaining thousands of distance measures.<sup>8,23</sup> While prior DM studies have focused solely on distances between opposing articular surfaces, in this study, we adapt DMs to create novel clinically applicable coverage maps (CMs) that also identify the entire 3D extent of joint subluxation and bony impingement. We hypothesized that, compared to controls, CM assessment would demonstrate significantly decreased joint coverage of all SJ articular facets in patients with PCFD that would be more pronounced at the middle facet. We further hypothesized that decreased interbone distances would be found in the sinus tarsi and subfibular regions of patients with PCFD, consistent with impingement.

## Methods

This study obtained institutional review board approval before its start and complied with the Health Insurance Portability and Accountability Act (HIPAA).

### Study Design

A retrospective review of patient data collected between 2014 and 2020 was conducted to identify patients with clinical and radiographic diagnosis of PCFD who underwent a WBCT examination. Using the recently reported consensus statement new classification system by Myerson et al,<sup>27</sup> where stage I represents any flexible deformity (former

stage II by Johnson and Strom<sup>19</sup> and Myerson<sup>26</sup>), the first consecutive 20 patients in our WBCT data set with symptomatic stage I flexible PCFD<sup>27</sup> who had not undergone prior surgery of the affected foot and ankle were selected for the study. Patients were excluded for prior fracture, surgical treatment of the deformity, ankle/subtalar arthritis, or rigid deformity. Patients with PCFD with any combination of deformities comprised by classes A, B, C, and/or D were included.<sup>27</sup> Patients with class E deformity (valgus ankle tilt/deltoid insufficiency) were not included.<sup>27</sup> A group of 10 control patients who had no clinical or WBCT signs of PCFD or hallux valgus, had no major deformities or prior foot and ankle surgical procedures, and underwent bilateral WBCT examination for unilateral foot and ankle pathologies were matched to have similar distributions of age, sex, and body mass index (BMI). Scans were obtained to evaluate the contralateral foot and ankle for the following conditions: ankle pain (2), midfoot sprain, distal fibular fracture (3), loose bodies in the ankle, lateral ankle instability, proximal fifth metatarsal fracture, and plantar plate injury of a lesser toe.

### Image Acquisition

WBCT studies were performed with a cone-beam computed tomography (CT) scanner (PedCAT; Curvebeam). Participants were instructed to bear weight in a natural, upright standing position with the feet approximately at shoulder width and to distribute body weight evenly between the 2 lower limbs.

### 3D Distance Mapping

Creation of DMs began with a semiautomated segmentation protocol that extracted the boundaries of the talus, calcaneus, and fibula from WBCT images using MATLAB code (The MathWorks). Segmentations were reviewed by a PhD-trained expert with over 7 years of experience. Resulting surfaces were exported as triangulated surface models to Geomagic Design X (3D Systems), in which they were smoothed to remove voxelation artifacts.

Distance measurements were performed along the entire superior surface of the calcaneus, including the SJ articular facets (anterior, middle, and posterior), sinus tarsi, and subfibular regions. For a more sectorized and detailed analysis, the SJ posterior facet was divided into a 3 × 3 grid using the principal axes of the joint surface while the sinus tarsi was divided into quadrants: anteromedial, anterolateral, posteromedial, and posterolateral (Figure 1). Measurements performed in SJ articular areas were defined as the distance along the normal direction of vectors projected from the calcaneal subchondral surface to the opposed surface of the talus (normal distance). Force is primarily transferred between surfaces along a direction normal to contact, so the

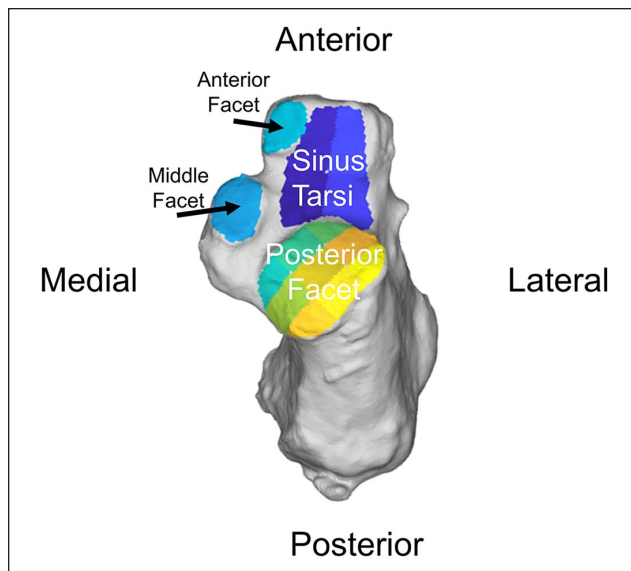


**Figure 1.** Superior view of the calcaneus showing regional divisions used in the analyses.

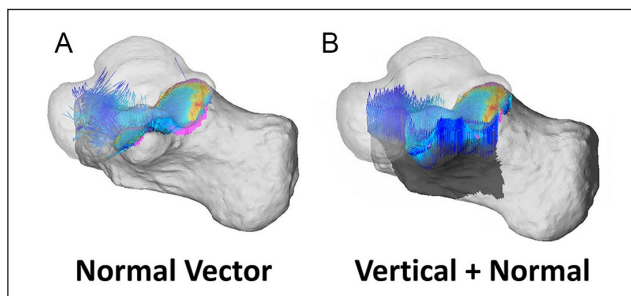


**Figure 2.** Distance mapping was performed using normal vectors in articular regions and vertical vectors in noncontacting, nonarticular regions. (A) Example where distances between surfaces along normal vectors in noncontacting regions can result in highly irregular measurements that do not identify meaningful patterns of coverage between surfaces. (B) Example where the use of vertical vectors in irregular noncontacting regions identifies more meaningful patterns of coverage.

normal distances in contacting (articular) regions would provide measurements along a vector closely related to the direction experiencing the greatest compression under loading. However, in nonarticular regions like the sinus tarsi and subfibular areas, surfaces can be highly curved and produce aberrantly large normal distances unrelated to loading and deviating significantly from neighboring regions (Figure 2A). Therefore, to provide more accurate measures in highly curved/uneven nonarticular surfaces, distances were computed as the vertical distance from each point to the opposed surface based on the scanner's coordinate system (Figure 2B). DMs were then created from all individual distance measurements. The posterior, middle, and anterior

(when distinct) SJ facets were semiautomatically identified in each data set by a PhD-trained expert based on changes in curvature at the edge of subchondral bone regions using Geomagic Design X (3D Systems). Anterior facets that were confluent with the middle facet were considered together as a single, large middle facet in the results. The sinus tarsi region was manually identified while subfibular regions were automatically identified using DMs. Subluxation was quantified on the articular facets as the percentage of joint uncoverage defined as the area not covered by the talus divided by the entire area of each calcaneal articular facet.

DMs were colored to highlight regions of interest (Figure 3A). Covered regions with distances greater than 4 mm were therefore shown in gray to indicate shadows in noncontacting regions as prior literature has shown that subchondral bone-to-bone distances rarely exceed 3 mm in the SJ.<sup>8,23</sup> Regions with distances from 1 to 4 mm were shown in blue to indicate expected joint interaction. Distances under 1 mm were highlighted with colors from yellow to red indicating close bone proximity consistent with joint space narrowing or impingement in these regions.

### Coverage Maps

Colored CMs were created using the measured DMs to better highlight areas of adequate joint interaction, joint subluxation, and impingement. Pink was chosen to highlight uncoverage of SJ articular regions, as a result of the overall 3D deformity in PCFD, that were either completely uncovered or had distances greater than 4 mm (Figure 3B). Red was chosen to indicate close bone interaction, consistent with extra-articular bony impingement. For this, we used DM values of less than 0.5 mm, our largest voxel size, providing an objective definition of impingement that did not rely on indirect signs like sclerosis or cysts.<sup>24</sup> Blue was chosen to indicate regions where joint and peritalar interactions (DMs) were found to be between 0.5 mm (no impingement) and 4 mm. The 4-mm upper threshold was chosen based on prior literature that demonstrated cartilage thickness and bone-to-bone distances rarely exceed 3 mm in the SJ.<sup>8,23</sup> Finally, gray was used to indicate a shadow from the talus in nonarticular regions of the calcaneus, where DMs were greater than 4 mm.

### Statistical Analysis

Descriptive statistics of mean, standard deviation, and range were reported for the distance maps and coverage areas in each region. Raw data were initially checked for normality using the Shapiro-Wilk *W* test. Two-tailed independent samples Student *t* tests or Wilcoxon tests were used to assess differences between control and PCFD groups, depending on the normality of their distributions. Statistical

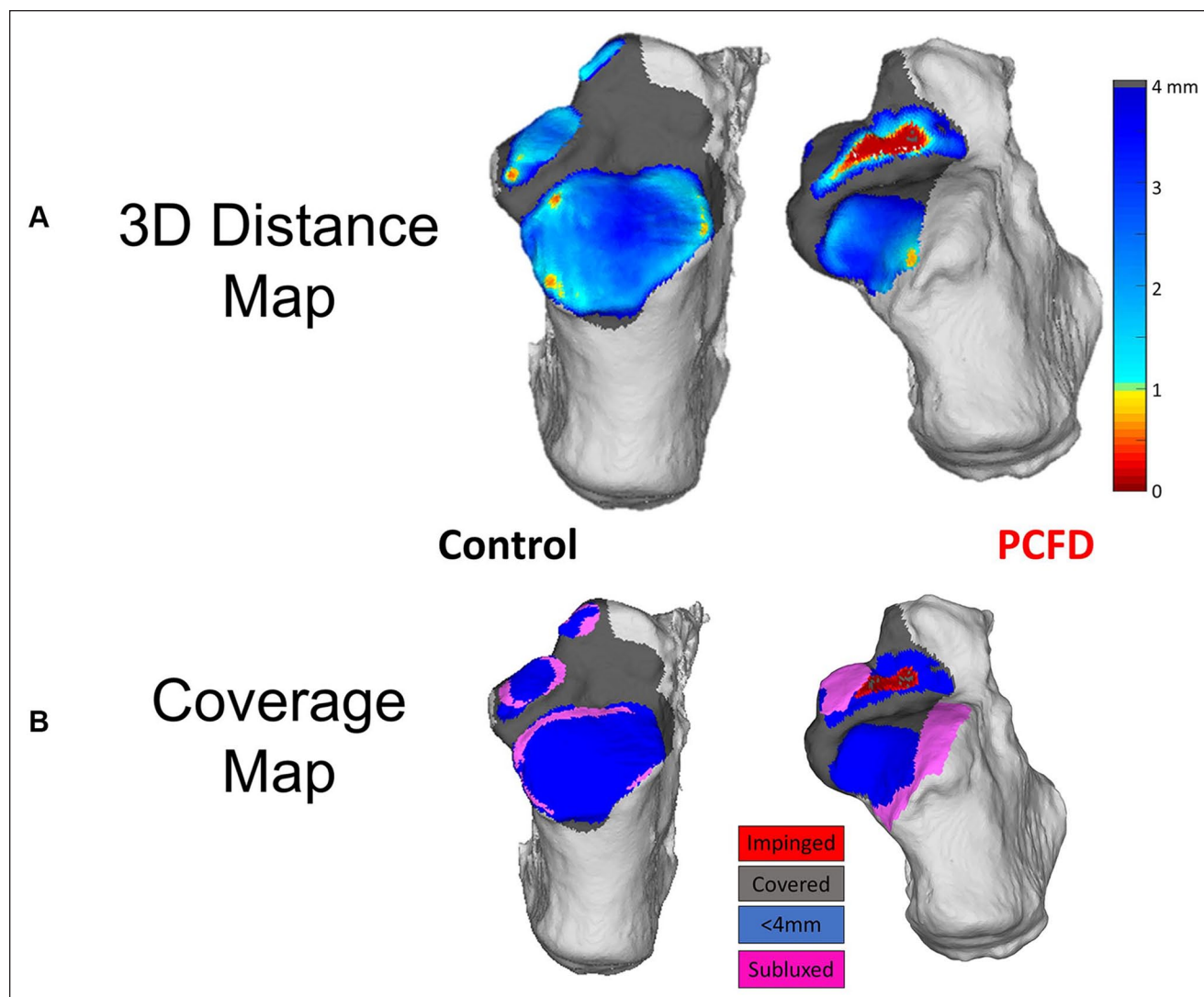


**Figure 3.** Comparisons of distance maps (DMs) between patients with progressive collapsing foot deformity (PCFD) and control patients identify differences between patients, but important areas of subluxation are more clearly identified on coverage maps (CMs). (A) A comparison of raw DMs for a patient with PCFD and a control patient highlights potential regions of impingement. (B) CMs clearly identify regions of subluxation, coverage, and impingement and draw attention to these clinically important features.

analysis was performed by an independent observer using a dedicated software (JMP Pro, 15.0.0; SAS Institute). *P* values of .05 or lower were considered significant.

## Results

There were no significant differences in patient characteristics between the PCFD and control groups with respect to age ( $P = .92$ ), sex ( $P = 1.00$ ), and BMI ( $P = .40$ ) distributions (Table 1).

A summary of mean and minimum DMs measurements is reported, respectively, in Tables 2 and 3. No significant differences in the mean distances between any articular surface or subregion were found, although consistent increases in middle facet DMs were demonstrated (29.4%,  $P = .054$ ).

Significant increases in minimum distances were identified only in the anterior facet (126%,  $P < .03$ ), although the middle facet again showed a similar trend (53.4%,  $P = .08$ ) (Table 3).

Overall, coverage was decreased in articular regions of the SJ, and areas of impingement were increased in non-articular regions (sinus tarsi and subfibular areas) of patients with PCFD compared to controls (Table 4). Figure 4 demonstrates the differences in coverage between a typical control and PCFD patient. These differences can be seen systematically in Figure 5, in which coverage maps are shown for all patients with PCFD and controls.

A summary of joint and peritalar coverage can be found in Table 4. When compared to controls, there was a significant increase in joint uncoverage of the SJ middle facet



**Table 1.** Progressive Collapsing Foot Deformity and Control Patients' Demographics.

Characteristic	PCFD (n = 20)	Control (n = 10)	P value
Male, No.	8	4	—
Female, No.	12	6	—
Age, mean $\pm$ SD, y	40.9 $\pm$ 17.8	40.2 $\pm$ 15.6	.92
BMI, mean $\pm$ SD, kg/m <sup>2</sup>	32.7 $\pm$ 8.2	35.5 $\pm$ 8.1	.40

Abbreviations: BMI, body mass index; PCFD, progressive collapsing foot deformity; —, no entries for statistical comparison.

**Table 2.** Means and Standard Deviations for 3-Dimensional Distance Maps, Measured in Millimeters, and Mean Differences in the Distances When Comparing Patients With Progressive Collapsing Foot Deformity and Controls, With P Values and 95% CIs for the Comparisons.<sup>a</sup>

Characteristic	Control, mm		PCFD, mm		Mean difference, %	P value	95% CI	
	Mean	SD	Mean	SD				
Anterior facet	1.98	0.59	2.66	0.73	34.5	.126	-1.53	0.16
Middle facet	1.36	0.36	1.77	0.71	29.5	.113	-0.81	0.01
Posterior facet	1.74	0.44	1.90	0.43	9.6	.322	-0.54	0.21
Sinus tarsi	2.73	0.39	2.63	0.67	-3.6	.481	-0.31	0.51
Posterior facet								
Anterior								
Medial	2.22	0.69	2.11	0.45	-5.0	.846	-0.43	0.66
Middle	2.01	0.53	2.23	0.43	10.6	.397	-0.65	0.22
Lateral	1.62	0.43	1.99	0.71	22.5	.091	-0.81	0.08
Middle								
Medial	1.72	0.65	1.77	0.59	3.2	.779	-0.60	0.49
Middle	2.03	0.58	2.14	0.47	5.4	.588	-0.58	0.36
Lateral	1.44	0.44	1.78	0.63	24.1	.100	-0.77	0.08
Posterior								
Medial	1.31	0.42	1.18	0.45	-10.4	.475	-0.23	0.50
Middle	1.72	0.46	1.62	0.55	-5.9	.502	-0.31	0.51
Lateral	1.43	0.50	1.80	0.70	26.0	.151	-0.85	0.11
Sinus tarsi								
Anterior								
Medial	5.52	2.17	4.11	1.41	-25.6	.098	-0.30	3.13
Lateral	<b>7.78</b>	<b>1.50</b>	<b>5.60</b>	<b>2.20</b>	<b>-28.1</b>	<b>.022</b>	<b>0.56</b>	<b>3.82</b>
Posterior								
Medial	<b>6.19</b>	<b>0.92</b>	<b>4.04</b>	<b>1.22</b>	<b>-34.8</b>	<b>&lt;.001</b>	<b>1.30</b>	<b>3.01</b>
Lateral	<b>7.81</b>	<b>2.05</b>	<b>5.96</b>	<b>1.88</b>	<b>-23.7</b>	<b>.031</b>	<b>0.13</b>	<b>3.57</b>
Subfibular	<b>20.05</b>	<b>1.77</b>	<b>17.01</b>	<b>1.96</b>	<b>-15.1</b>	<b>&lt;.001</b>	<b>1.49</b>	<b>4.58</b>

Abbreviation: PCFD, progressive collapsing foot deformity.

<sup>a</sup>Bolded rows denote significant changes within the region.

of patients with PCFD (46.6%,  $P < .001$ ) but not anterior or posterior facets (Table 4). The anterior facet was confluent with the middle facet in 4 of 10 controls and 5 of 20 patients with PCFD and was therefore not evaluated in isolation in these patients. When evaluated by subregion, decreases in posterior facet coverage were identified in midlateral and posterolateral regions, but these changes did not reach statistical significance ( $P = .24$ ,  $P = .08$ , respectively) (Figure 6).

Significant increases in overall coverage of the sinus tarsi region (98.0%,  $P < .007$ ) along with sinus tarsi impingement (DM  $< 0.5$  mm) were identified in 6 of 20 (30%) patients with PCFD and none of the controls (Table 4). Impingement of the subfibular region (Figure 7) was noted in only 1 of 20 (5%) of PCFD cases, but narrowing of the distance between the fibula and calcaneus that was 2 standard deviations greater than the average observed in controls was noted in 17 of 20 (85%) of patients with

**Table 3.** Minimum Value and Standard Deviations for 3-Dimensional Distance Maps, Measured in Millimeters, and Mean Differences in the Distances When Comparing Patients With Progressive Collapsing Foot Deformity and Controls, With *P* Values and 95% CIs for the Comparisons.<sup>a</sup>

Characteristic	Control, mm		PCFD, mm		Mean difference, %	<i>P</i> value	95% CI	
	M	SD	M	SD				
Anterior facet	<b>0.82</b>	<b>0.58</b>	<b>1.86</b>	<b>0.97</b>	<b>126.7</b>	<b>.027</b>	<b>-1.96</b>	<b>-0.12</b>
Middle facet	0.68	0.42	1.05	0.66	54.0	.135	-0.79	0.05
Posterior facet	0.42	0.33	0.36	0.35	-13.9	.674	-0.23	0.35
Sinus tarsi	1.34	0.74	1.25	1.18	-6.8	.804	-0.66	0.85
Posterior facet								
Anterior								
Medial	1.33	0.85	1.29	0.53	-2.8	.906	-0.63	0.71
Middle	1.29	0.62	1.35	0.51	5.0	.650	-0.57	0.44
Lateral	0.91	0.46	1.31	0.65	43.3	.100	-0.84	0.05
Middle								
Medial	0.68	0.57	0.95	0.50	39.3	.131	-0.74	0.20
Middle	1.41	0.58	1.35	0.58	-3.8	.681	-0.44	0.55
Lateral	0.61	0.35	0.91	0.58	49.4	.183	-0.67	0.07
Posterior								
Medial	0.58	0.41	0.56	0.50	-3.6	.908	-0.35	0.39
Middle	1.06	0.42	0.73	0.60	-30.8	.082	-0.08	0.73
Lateral	0.84	0.60	1.34	0.69	60.3	.077	-1.04	0.03
Sinus tarsi								
Anterior								
Medial	2.81	2.76	1.68	1.27	-40.1	.269	-1.00	3.25
Lateral	<b>6.30</b>	<b>2.89</b>	<b>3.54</b>	<b>2.34</b>	<b>-43.7</b>	<b>.035</b>	<b>0.05</b>	<b>5.47</b>
Posterior								
Medial	<b>2.60</b>	<b>0.75</b>	<b>1.53</b>	<b>1.30</b>	<b>-41.2</b>	<b>.031</b>	<b>0.28</b>	<b>1.87</b>
Lateral	<b>5.81</b>	<b>3.14</b>	<b>3.04</b>	<b>2.18</b>	<b>-47.7</b>	<b>.027</b>	<b>0.26</b>	<b>5.29</b>
Subfibular	<b>10.64</b>	<b>1.16</b>	<b>6.02</b>	<b>2.61</b>	<b>-43.4</b>	<b>&lt;.001</b>	<b>3.16</b>	<b>6.08</b>

Abbreviations: M, minimum distance averaged within control and PCFD patient groups for each region specified; PCFD, progressive collapsing foot deformity.

<sup>a</sup>Bolded rows denote significant changes within the region.

PCFD (Table 3). No control patients demonstrated similar decreases in calcaneofibular distances.

## Discussion

In this case-control study with stage I flexible patients with PCFD, we evaluated joint subluxation and impingement associated with PTS across the entire SJ surface using WBCT images, DM, and CM. We objectively identified middle facet subluxation as the only consistent significant marker of PTS, with an average increase in subluxation of 46% in patients with PCFD compared to controls. We present a color-guided method to facilitate the interpretation of DMs and created CMs to automatically identify areas of extra-articular impingement and SJ subluxation. To our knowledge, this is the first time a true 3D analysis of the entire extension of the SJ was performed using standing, upright, weightbearing CT in patients with PCFD.

Although recent studies have suggested that middle facet subluxation may provide an earlier marker of PTS, subluxation of the posterior facet is the present gold standard.<sup>16,17</sup> The methods used in this study enabled objective measurement of the true 3D nature of subluxation across the entire peritalar surface and, consequently, comparison between subluxation of the anterior, middle, and posterior facets. All measures in the posterior facet regions failed to reach significance, while differences in the anterior facet were inconsistent with wide confidence intervals. In contrast, the middle facet showed consistent and highly significant increases in uncoverage over 46.6% ( $P < .001$ ) and narrower confidence intervals supporting recent findings in the literature that the middle facet may provide a more robust and possibly earlier marker of PTS.<sup>10,14</sup> Considering the multiplanar characteristics of PCFD, where a combination of external rotation, valgus, and lateral translation of the calcaneus underneath the talus occurs during PTS,<sup>1,2,20,22</sup> a possible explanation for the lack of subluxation findings in

**Table 4.** Mean Coverage and Standard Deviations for 3-Dimensional Distance Maps, Measured as a Percentage, and Mean Differences in the Coverages When Comparing Patients With Progressive Collapsing Foot Deformity and Controls, With *P* Values and 95% CIs for the Comparisons.<sup>a</sup>

Characteristic	Control, mm		PCFD, mm		Mean difference, %	<i>P</i> value	95% CI	
	Mean	SD	Mean	SD				
Anterior facet	0.18	0.10	0.09	0.11	-48.9	.118	-0.03	0.21
Middle facet	<b>0.76</b>	<b>0.13</b>	<b>0.41</b>	<b>0.22</b>	<b>-46.6</b>	<b>&gt;.001</b>	<b>0.22</b>	<b>0.49</b>
Posterior facet	0.82	0.08	0.78	0.07	-5.9	.120	-0.02	0.11
Sinus tarsi	<b>0.15</b>	<b>0.10</b>	<b>0.30</b>	<b>0.17</b>	<b>98.0</b>	<b>.022</b>	<b>-0.26</b>	<b>-0.05</b>
Posterior facet								
Anterior								
Medial	0.63	0.31	0.72	0.19	13.2	.746	-0.33	0.16
Middle	0.93	0.09	0.99	0.03	6.1	.056	-0.12	0.01
Lateral	0.96	0.06	0.93	0.11	-2.8	1.000	-0.04	0.09
Middle								
Medial	0.80	0.15	0.74	0.12	-7.4	.198	-0.06	0.18
Middle	1.00	0.00	1.00	0.00	0.0	.525	0.00	0.00
Lateral	0.92	0.08	0.86	0.13	-6.8	.241	-0.02	0.15
Posterior								
Medial	0.71	0.23	0.57	0.27	-20.4	.214	-0.06	0.35
Middle	0.74	0.18	0.69	0.20	-7.7	.454	-0.10	0.21
Lateral	0.49	0.33	0.29	0.23	-41.5	.082	-0.06	0.46
Sinus tarsi								
Anterior								
Medial	0.31	0.29	0.45	0.33	45.6	.262	-0.40	0.11
Lateral	0.02	0.04	0.09	0.16	297.8	.063	-0.14	0.02
Posterior								
Medial	<b>0.19</b>	<b>0.16</b>	<b>0.54</b>	<b>0.28</b>	<b>183.6</b>	<b>.004</b>	<b>-0.52</b>	<b>-0.18</b>
Lateral	0.07	0.14	0.15	0.20	98.9	.136	-0.21	0.06

Abbreviation: PCFD, progressive collapsing foot deformity.

<sup>a</sup>Bolded rows denote significant changes within the region.

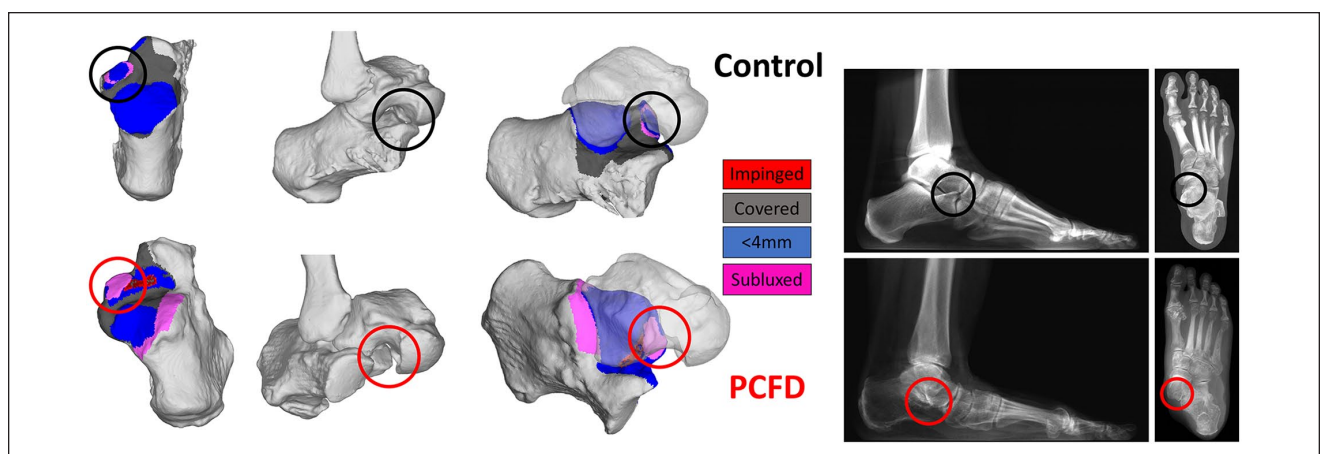


**Figure 4.** Comparison of 3-dimensional coverage, radiographs, and coverage maps between a representative control (top) and progressive collapsing foot deformity (PCFD) patient (bottom). The circles identify the middle facet on, respectively, coverage maps of a superior view of the calcaneal peritarsal surface (left), lateral view of the hindfoot (middle), and lateral view showing same coverage maps and the relationship of talus and calcaneus (right).

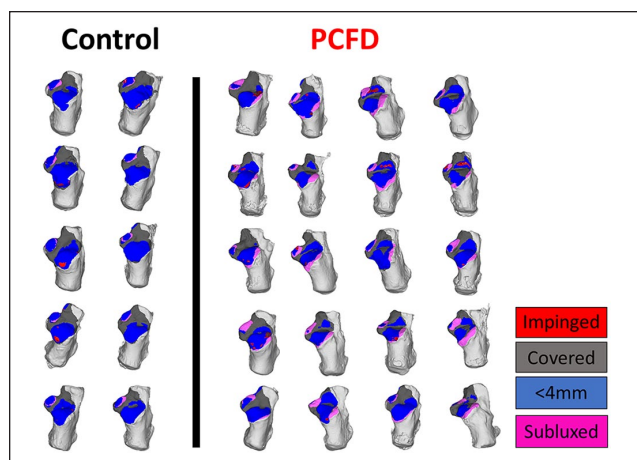


**Figure 5.** Coverage maps of all cases included in the study identifying regions of subluxation, impingement, and normal coverage. PCFD, progressive collapsing foot deformity.

the posterior facet is that the rotational component of the deformity occurs within the natural bounds of posterior facet articulation, closer to the center of rotation of the deformity and resulting in less joint uncoverage.<sup>10,14</sup> Therefore, quantifying PTS at the middle facet may provide the optimal tool to detect early PCFD progression and potentially optimize decision making on ideal timing for interventions.

Concordantly, CMs also indicated substantial increases in coverage (98.0%,  $P < .001$ ) of the sinus tarsi region, a recognized area of impingement and lateral hindfoot pain in patients with PCFD. Increased coverage and impingement in this region is explained by external rotation and eversion of the calcaneus underneath the talus, with closure of the sinus tarsi area and Gissane angle of the calcaneus, which is filled by the lateral process of the talus, leading to bone-on-bone and soft tissue impingement.<sup>10</sup> Although we found impingement at much lower rates than previously reported (30% vs 92% sinus tarsi impingement and 5% vs 66% calcaneofibular impingement),<sup>24</sup> the differences are likely related to our objective analyses identifying direct contact of bones rather than indirect and potentially more subjective signs of impingement, such as the presence of cysts and sclerosis, that were previously used in the literature.<sup>24</sup> However, definitive narrowing, as demonstrated by decreased DMs, was found in 17 of 20 subfibular regions in patients with PCFD, potentially providing another indicator of progressive deformity.

One of the more surprising findings was that SJ anterior facet coverage was lower than 20%, even in control patients. We attribute this finding to the anatomically variable nature of the anterior facet interface with the talus,<sup>4</sup> with an inconsistent interface resulting in uncoverage during standing. Further study will be required to determine if this lack of coverage is indicative of asymptomatic subluxation. Considering the purpose of this study, these results lead us to

conclude that the anterior facet is not a reliable indicator of PTS and subsequently a poor marker for progressive PCFD.

Similarly, SJ middle and posterior facets showed lower coverage in healthy controls than previously reported in the literature, at 75.9% and 82.5%, respectively.<sup>1,10,14</sup> Ananthakrishnan et al<sup>1</sup> previously reported 95% and 92% coverage in control patients' combined anterior/middle and posterior facets, respectively. The relatively lower coverage we report is likely attributable to true weightbearing resulting in more subluxation when compared to the 75 N (~10% body-weight) loading applied previously.<sup>1</sup> For more recent studies using the full weightbearing techniques, improved 3D measures of coverage can explain the difference. Prior coronal plane 2D measures at the anteroposterior midpoint of the joint do not account for coverage gaps existing around the periphery of the larger calcaneal surface that our 3D measures capture.<sup>10,14</sup> Future studies with larger control cohorts will be needed to more definitively establish normal coverage ranges.

This study had several limitations. First, controls were selected from patients with contralateral foot and ankle injuries and deformities. Therefore, subtle asymmetries resulting from antalgic stance may confound results. We acknowledge that a direct matching process with healthy normal volunteer controls would improve the quality of the data collected. However, we believe it would be unlikely to have a notable impact on the DM findings. Second, only patients with stage I flexible PCFD were evaluated. Future work should study the full range of possible PCFD deformities, including stages I and II, as well as analyzing the different classes (A, B, C, D, and E) separately. Third, we did not compare the findings with traditional 2D coronal plane measures of SJ subluxation or other classic PCFD measurements. We would expect significant correlation between them, and comparisons should be included in future investigations. In addition, the high BMI in this data set may have resulted in larger deformities and subluxation during weightbearing than seen in a lower BMI cohort. It may also have affected normal alignment in the controls. However, given the clear differences identified and similarity to prior findings, we do not believe this had a meaningful impact on results. Another limitation is that the images were taken in quiet standing and static images—in any position—do not tell a dynamic story. Other parts of the gait cycle may add stress and greater displacement of topologies analyzed. Additionally, we did not assess clinical outcomes in our study or correlate them with deformity progression, limiting the immediate clinical implications of our findings. For future prospective and longitudinal investigations, it is critical that we determine the role of middle facet subluxation in relation to clinical and patient-reported outcomes as well as in deformity progression and surgical deformity correction in patients with PCFD. Finally, no formal power analysis was performed, and our sample could be underpowered to demonstrate differences in some of the measurements performed. However, the significant and considerable



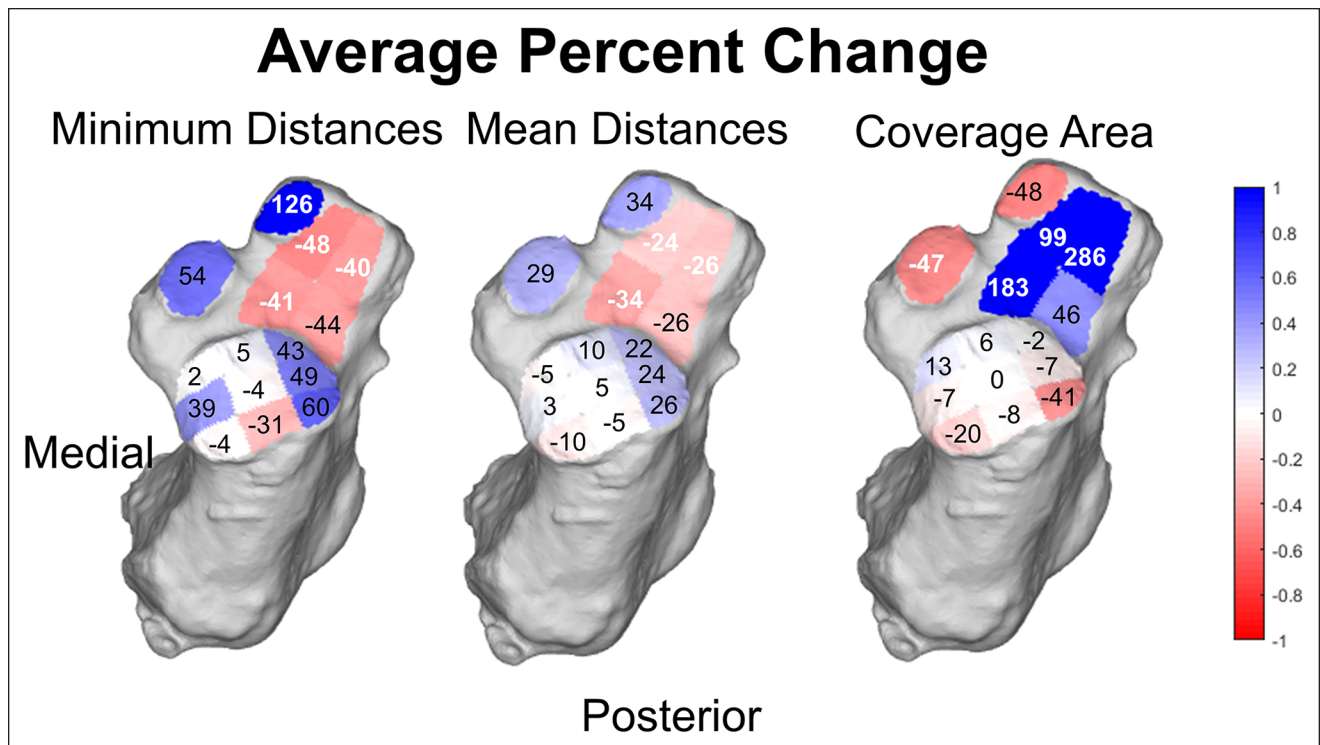


**Figure 6.** Superior view of a representative calcaneus showing average percentage change in minimum (left) and mean (middle) distances as well as the average percent change in coverage area for all cases. Significant differences are shown with a bolded white color.

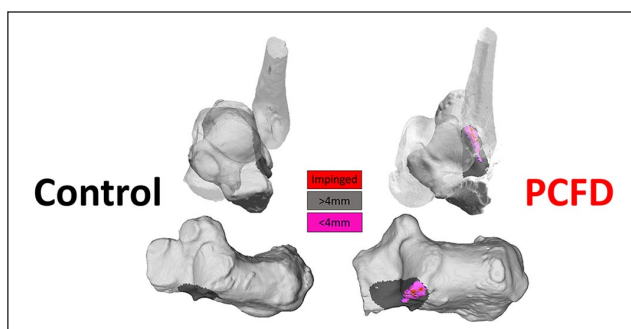


**Figure 7.** Subfibular impingement identified by distance maps (DMs) occurring in a patient with progressive collapsing foot deformity (PCFD) compared to the DM of a control.

differences found in middle facet uncoverage indicate the sample size was sufficient to evaluate key findings.

In summary, novel WBCT distance map and coverage map techniques were applied in patients with PCFD and controls to objectively quantify 3D subtalar joint coverage, sinus tarsi, and subfibular impingements as markers of PTS. When comparing uncoverage of the SJ posterior, middle, and anterior facets as markers of PTS, only the middle facet was found to be a consistent and significant predictor of pronounced PTS. CMs were also able to identify significant changes related to sinus tarsi and subfibular impingement

that may be responsible for lateral-sided pain associated with PCFD. Importantly, we also introduced more interpretable and potentially clinically useful colored coverage maps that highlighted areas of interest where subluxation and impingement occur to facilitate the understanding of the degree of PTS in PCFD.

Although subluxation of the subtalar joint as a marker of PTS in patients with PCFD has been well described in the literature, the results of this study strongly and 3-dimensionally support the middle facet as the earliest and most accurate marker for symptomatic and pronounced deformity. Rapid developments in low-cost, low-dose WBCT imaging, combined with those in automated 3D analyses, should bring advanced analyses like these to the clinical setting. Our hope is that DM and CM assessment of SJ middle facet subluxation in WBCT images can represent an objective, reliable, and accurate diagnostic tool to predict patients with higher risk of progressive collapse, considering that recent data demonstrated that the subluxation of the middle facet is significantly correlated with the overall 3D deformity severity in PCFD.<sup>14</sup> Therefore, the data collected in the current study, using robust and objective 3D measures, could shine light and support further investigations to optimize early intervention in patients with PCFD, aiming to halt deformity progression and hindfoot joint degeneration.<sup>14</sup> Longitudinal and prospective studies are now needed to confirm

the findings of this study and correlate them with deformity progression and clinical outcomes, searching for threshold values of middle facet subluxation that could predict worsening of outcomes and need for more aggressive interventions.

## Conclusion

In conclusion, our study results revealed that compared to controls, patients with PCFD demonstrated that a significant decrease in 3D measures of subtalar joint coverage was identified only in the middle facet but not in the anterior or posterior facets. We also determined significantly decreased interbone distances in the sinus tarsi and subfibular regions of patients with PCFD, confirming the occurrence of extra-articular impingement in those areas. We hope that the use of these 3D accurate and objective new measures of DM and CM of middle facet subluxation will support the early detection of patients with PCFD at high risk for collapse and assist with clinical decision making with respect to which patients will require or be spared a hindfoot fusion procedure as a part of their surgical treatment.

## Declaration of Conflicting Interests

The author(s) declared the following potential conflicts of interest with respect to the research, authorship, and/or publication of this article: Francois Lintz, MD, MSc, FEBOT, reports personal fees, nonfinancial support, and other from Curvebeam LLC during the conduct of the study and is cofounder and vice president of the International Weight Bearing CT Society. Cesar de Cesar Netto, MD, PhD, reports grants, personal fees, and other from CurveBeam and is treasurer of the International Weight Bearing CT Society. ICMJE forms for all authors are available online.

## Funding


The author(s) received no financial support for the research, authorship, and/or publication of this article.

## ORCID iDs

Kevin N. Dibbern, PhD,  <https://orcid.org/0000-0002-8061-4453>

Francois Lintz, MD, MSc, FEBOT,  <https://orcid.org/0000-0002-0163-6516>

Scott J. Ellis, MD,  <https://orcid.org/0000-0002-4304-7445>

Cesar de Cesar Netto, MD, PhD,  <https://orcid.org/0000-0001-6037-0685>

## References

1. Ananthakrishnan D, Ching R, Tencer A, Hansen ST Jr, Sangeorzan BJ. Subluxation of the talocalcaneal joint in adults who have symptomatic flatfoot. *J Bone Joint Surg Am*. 1999;81(8):1147-1154.
2. Anderson JG, Harrington R, Ching RP, Tencer A, Sangeorzan BJ. Alterations in talar morphology associated with adult flatfoot. *Foot Ankle Int*. 1997;18(11):705-709.
3. Apostle KL, Coleman NW, Sangeorzan BJ. Subtalar joint axis in patients with symptomatic peritalar subluxation compared to normal controls. *Foot Ankle Int*. 2014;35(11):1153-1158.
4. Bunning PS, Barnett CH. A Comparison of adult and foetal talocalcaneal articulations. *J Anat*. 1965;99:71-76.
5. Carrino JA, Al Muhit A, Zbijewski W, et al. Dedicated cone-beam CT system for extremity imaging. *Radiology*. 2014;270(3):816-824.
6. Cody EA, Williamson ER, Burket JC, Deland JT, Ellis SJ. Correlation of talar anatomy and subtalar joint alignment on weightbearing computed tomography with radiographic flat-foot parameters. *Foot Ankle Int*. 2016;37(8):874-881.
7. Colin F, Horn Lang T, Zwicky L, Hintermann B, Knupp M. Subtalar joint configuration on weightbearing CT scan. *Foot Ankle Int*. 2014;35(10):1057-1062.
8. Day MA, Ho M, Dibbern K, et al. Correlation of 3D joint space width from weightbearing CT with outcomes after intra-articular calcaneal fracture. *Foot Ankle Int*. 2020;41(9):1106-1116.
9. de Cesar Netto C, Deland JT, Ellis SJ. Guest editorial: expert consensus on adult-acquired flatfoot deformity. *Foot Ankle Int*. 2020;41(10):1269-1271.
10. de Cesar Netto C, Godoy-Santos AL, Saito GH, et al. Subluxation of the middle facet of the subtalar joint as a marker of peritalar subluxation in adult acquired flatfoot deformity: a case-control study. *J Bone Joint Surg Am*. 2019;101(20):1838-1844.
11. de Cesar Netto C, Myerson MS, Day J, et al. Consensus for the use of weightbearing CT in the assessment of progressive collapsing foot deformity. *Foot Ankle Int*. 2020;41(10):1277-1282.
12. de Cesar Netto C, Schon LC, Thawait GK, et al. Flexible adult acquired flatfoot deformity: comparison between weight-bearing and non-weight-bearing measurements using cone-beam computed tomography. *J Bone Joint Surg Am*. 2017;99(18):e98.
13. de Cesar Netto C, Shakoore D, Dein EJ, et al. Influence of investigator experience on reliability of adult acquired flatfoot deformity measurements using weightbearing computed tomography. *Foot Ankle Surg*. 2019;25(4):495-502.
14. de Cesar Netto C, Silva T, Li S, et al. Assessment of posterior and middle facet subluxation of the subtalar joint in progressive flatfoot deformity. *Foot Ankle Int*. 2020;41(10):1190-1197.
15. Deland JT. Adult-acquired flatfoot deformity. *J Am Acad Orthop Surg*. 2008;16(7):399-406.
16. Ellis SJ, Deyer T, Williams BR, et al. Assessment of lateral hindfoot pain in acquired flatfoot deformity using weightbearing multiplanar imaging. *Foot Ankle Int*. 2010;31(5):361-371.
17. Ferri M, Scharfenberger AV, Goplen G, Daniels TR, Pearce D. Weightbearing CT scan of severe flexible pes planus deformities. *Foot Ankle Int*. 2008;29(2):199-204.
18. Haleem AM, Pavlov H, Bogner E, Sofka C, Deland JT, Ellis SJ. Comparison of deformity with respect to the talus in patients with posterior tibial tendon dysfunction and controls using multiplanar weight-bearing imaging or conventional radiography. *J Bone Joint Surg Am*. 2014;96(8):e63.
19. Johnson KA, Strom DE. Tibialis posterior tendon dysfunction. *Clin Orthop Relat Res*. 1989;239:196-206.

20. Kido M, Ikoma K, Imai K, et al. Load response of the tarsal bones in patients with flatfoot deformity: in vivo 3D study. *Foot Ankle Int.* 2011;32(11):1017-1022.
21. Kunas GC, Probasco W, Haleem AM, Burket JC, Williamson ERC, Ellis SJ. Evaluation of peritalar subluxation in adult acquired flatfoot deformity using computed tomography and weightbearing multiplanar imaging. *Foot Ankle Surg.* 2018;24(6):495-500.
22. Ledoux WR, Rohr ES, Ching RP, Sangeorzan BJ. Effect of foot shape on the three-dimensional position of foot bones. *J Orthop Res.* 2006;24(12):2176-2186.
23. Lintz F, Jepsen M, De Cesar Netto C, et al. Distance mapping of the foot and ankle joints using weightbearing CT: the cavovarus configuration [published online May 26, 2020]. *Foot Ankle Surg.*
24. Malicky ES, Crary JL, Houghton MJ, Agel J, Hansen ST Jr, Sangeorzan BJ. Talocalcaneal and subfibular impingement in symptomatic flatfoot in adults. *J Bone Joint Surg Am.* 2002;84(11):2005-2009.
25. Meehan RE, Brage M. Adult acquired flat foot deformity: clinical and radiographic examination. *Foot Ankle Clin.* 2003;8(3):431-452.
26. Myerson MS. Adult acquired flatfoot deformity: treatment of dysfunction of the posterior tibial tendon. *Instr Course Lect.* 1997;46:393-405.
27. Myerson MS, Thordarson DB, Johnson JE, et al. Classification and nomenclature: progressive collapsing foot deformity. *Foot Ankle Int.* 2020;41(10):1271-1276.
28. Probasco W, Haleem AM, Yu J, Sangeorzan BJ, Deland JT, Ellis SJ. Assessment of coronal plane subtalar joint alignment in peritalar subluxation via weight-bearing multiplanar imaging. *Foot Ankle Int.* 2015;36(3):302-309.
29. Sangeorzan BJ, Hintermann B, de Cesar Netto C, et al. Progressive collapsing foot deformity: consensus on goals for operative correction. *Foot Ankle Int.* 2020;41(10):1299-1302.
30. Toolan BC, Sangeorzan BJ, Hansen ST Jr. Complex reconstruction for the treatment of dorsolateral peritalar subluxation of the foot: early results after distraction arthrodesis of the calcaneocuboid joint in conjunction with stabilization of, and transfer of the flexor digitorum longus tendon to, the mid-foot to treat acquired pes planovalgus in adults. *J Bone Joint Surg Am.* 1999;81(11):1545-1560.
31. Younger AS, Sawatzky B, Dryden P. Radiographic assessment of adult flatfoot. *Foot Ankle Int.* 2005;26(10):820-825.